NIH Public Access
Author Manuscript
J Biol Chem. Author manuscript; available in PMC 2009 March 13.

Published in final edited form as:
J Biol Chem. 2007 October 5; 282(40): 29201–29210. doi:10.1074/jbc.M703458200.

$G\alpha_q$ Directly Activates p63RhoGEF and Trio via a Conserved Extension of the Dbl Homology-associated Pleckstrin Homology Domain

Rafael J. Rojas‡,[1], **Marielle E. Yohe**‡, **Svetlana Gershburg**‡, **Takeharu Kawano**§, **Tohru Kozasa**¶,[2], and **John Sondek**‡,‖,**,[3]

‡*Department of Pharmacology, University of North Carolina, Chapel Hill, North Carolina 27599*

§*Department of Anatomy and Cell Biology, University of Illinois, Chicago, Illinois 60612*

¶*Department of Pharmacology, University of Illinois, Chicago, Illinois 60612*

‖*Department of Biochemistry and Biophysics, University of North Carolina, Chapel Hill, North Carolina 27599*

***Department of Lineberger Comprehensive Cancer Center, University of North Carolina, Chapel Hill, North Carolina 27599*

Abstract

The coordinated cross-talk from heterotrimeric G proteins to Rho GTPases is essential during a variety of physiological processes. Emerging data suggest that members of the $G\alpha_{12/13}$ and $G\alpha_{q/11}$ families of heterotrimeric G proteins signal downstream to RhoA via distinct pathways. Although studies have elucidated mechanisms governing $G\alpha_{12/13}$-mediated RhoA activation, proteins that functionally couple $G\alpha_{q/11}$ to RhoA activation have remained elusive. Recently, the Dbl-family guanine nucleotide exchange factor (GEF) p63RhoGEF/GEFT has been described as a novel mediator of $G\alpha_{q/11}$ signaling to RhoA based on its ability to synergize with $G\alpha_{q/11}$ resulting in enhanced RhoA signaling in cells. We have used biochemical/biophysical approaches with purified protein components to better understand the mechanism by which activated $G\alpha_q$ directly engages and stimulates p63RhoGEF. Basally, p63RhoGEF is autoinhibited by the Dbl homology (DH)-associated pleckstrin homology (PH) domain; activated $G\alpha_q$ relieves this autoinhibition by interacting with a highly conserved C-terminal extension of the PH domain. This unique extension is conserved in the related Dbl-family members Trio and Kalirin and we show that the C-terminal Rho-specific DH-PH cassette of Trio is similarly activated by $G\alpha_q$.

Rho GTPases are integral regulators of gene transcription and actin cytoskeletal remodeling during many dynamic cellular processes (1,2). Signal transduction cascades mediated by Rho GTPases originate via the extracellular stimulation of transmembrane receptors such as G protein-coupled receptors (GPCRs), [4] receptor tyrosine kinases, cytokine receptors, and integrins. Of the 22 human Rho family members, RhoA, Rac1, and Cdc42 are the most characterized, stemming from their ability to induce striking changes in cellular morphology

[1]Supported by United States Army Medical Research and Materiel Command, Breast Cancer Research Program Grant DAMD17-03-1-0646.

[2]Supported by National Institutes of Health Grant R01 GM6145408.

[3]Supported by National Institutes of Health Grants P01-GM65533 and R01-GM62299.

To whom correspondence should be addressed: Dept. of Pharmacology, University of North Carolina, CB 7365, 1106 M.E.J. Bldg., Chapel Hill, NC 27599. Tel.: 919-966-7350; Fax: 919-966-5640; E-mail: sondek@med.unc.edu.

NIH-PA Author Manuscript
NIH-PA Author Manuscript
NIH-PA Author Manuscript

NIH-PA Author Manuscript

NIH-PA Author Manuscript

NIH-PA Author Manuscript

upon activation (3). Numerous studies have established that RhoA activation downstream of GPCRs is vital for a multitude of diverse physiological responses including cell migration (4), lipid metabolism (5), vascular smooth muscle cell contraction (6–8), and cell survival/apoptosis (9–12). GPCR-mediated activation of RhoA effectively couples signaling pathways mediated by two distinct groups of guanine nucleotide-binding proteins: the heterotrimeric Gα-subunits and the monomeric small GTPases. These two groups of G proteins share a universal mechanism for guanine nucleotide binding, GTP hydrolysis, and conformational switching between two discrete states: a GDP-bound inactive state and a GTP-bound active state (13). Guanine nucleotide exchange factors (GEFs) activate G proteins by promoting the release of bound GDP, allowing the subsequent binding of GTP. Active, GTP-bound G proteins can then interact with numerous downstream effector molecules, further propagating the signal initiated at the plasma membrane.

GPCRs function as GEFs for heterotrimeric Gα-subunits, whereas Dbl-family GEFs are the major class of exchange factors for Rho GTPases. Dbl-family GEFs are defined by the presence of a Dbl homology domain (DH domain), which is almost invariantly followed by a pleckstrin homology domain (PH domain) (14). The catalytic guanine nucleotide exchange activity resides entirely within the DH domain, although recent evidence indicates that the PH domain can function to fine-tune this exchange activity (15,16). Previous studies have focused on the DH-associated PH domain as a simple membrane targeting device, by virtue of its ability to bind phosphoinositides. However, emerging evidence suggests that PH domains may also play important regulatory roles by serving as protein-protein interaction modules (17).

The coordinated cross-talk from GPCR stimulation to RhoA activation is mediated by Dbl-family GEFs that are responsive to activated Gα-subunits. A growing body of literature implicates both $G\alpha_{12/13}$ and $G\alpha_{q/11}$ family members as upstream activators of RhoA (18–20). Moreover, members of the$G\alpha_{12/13}$ and $G\alpha_{q/11}$ families utilize distinct pathways to signal downstream to RhoA (21). RhoA activation downstream of the $G\alpha_{12/13}$ family is mediated by the p115 family members, which consists of p115-RhoGEF, PDZ-RhoGEF, and leukemia-associated RhoGEF. The p115 family members are directly activated by $G\alpha_{12/13}$ via a protein-protein interaction mediated by a highly divergent regulator of G protein signaling (RGS) domain, but are not activated by $G\alpha_{q/11}$ family members (22–25). $G\alpha_{q/11}$-coupled GPCRs can signal downstream to RhoA via a pathway distinct from $G\alpha_{12/13}$ and independent of the classically described $G\alpha_{q/11}$ effector phospholipase C-β (21,26–29). However, whereas numerous studies have elucidated mechanisms underlying $G\alpha_{12/13}$-mediated RhoA activation, the signaling pathways that couple $G\alpha_{q/11}$ to RhoA activation have remained elusive.

Recently, the Dbl-family member p63RhoGEF/GEFT has been described as a novel mediator of $G\alpha_{q/11}$ signaling to RhoA based on its ability to synergize with $G\alpha_{q/11}$ resulting in enhanced RhoA signaling (30). Using cell model systems, the authors clearly demonstrate that$G\alpha_{q/11}$-coupled GPCR activation or overexpression of activated mutants of $G\alpha_{q/11}$ enhance the ability for overexpressed p63RhoGEF to activate serum response factor-dependent gene reporters. Furthermore, using co-immunoprecipitation studies, the authors deduced that activated $G\alpha_{q/11}$ associates with the C-terminal half of p63RhoGEF, which contains the PH domain. However, the mechanistic aspects underlying $G\alpha_{q/11}$-mediated p63RhoGEF activation remain unclear. In particular, the previous co-immunoprecipitation studies do not rule out the indirect association of$G\alpha_{q/11}$ with p63RhoGEF through ancillary proteins. Furthermore, it is necessary to determine whether $G\alpha_{q/11}$ can directly modulate the guanine nucleotide exchange activity of p63RhoGEF using a defined *in vitro* system. Here we use biochemical/ biophysical

[4]The abbreviations used are: GPCR, G protein-coupled receptor; GEF, guanine nucleotide exchange factor; DH, Dbl homology; PH, pleckstrin homology; RGS, regulator of G protein signaling; TEV, tobacco etch virus; MBP, maltose-binding protein; GST, glutathione S-transferase; SPR, surface plasmon resonance.

NIH-PA Author Manuscript
NIH-PA Author Manuscript
NIH-PA Author Manuscript

approaches with highly purified protein components to show that p63RhoGEF directly and specifically associates with activated $G\alpha_q$ to enhance robustly the catalyzed guanine nucleotide exchange of RhoA, RhoB, and RhoC. Therefore, p63RhoGEF is a *bona fide* effector of $G\alpha_q$. Furthermore, these studies strongly implicate p63RhoGEF, together with the related Dbl-family members, Trio and Kalirin, as a major nexus for the activation of RhoA downstream of $G\alpha_{q/11}$.

EXPERIMENTAL PROCEDURES

Molecular Constructs

Truncation mutant constructs of human p63RhoGEF were PCR amplified from full-length human p63RhoGEF (GenBank accession number BC012860, kindly provided by T. Wieland) resulting in the following constructs: DH-Ct (residues 155–580), DH-Ext (residues 155– 493), DH-PH (residues 155–472), and DH (residues 155–347). PCR products were then subcloned into a modified pET-21a vector (Novagen) using a previously published ligation-independent cloning strategy (31). The bacterial expression vector, pLiC-His-TEV, which encodes an N-terminal His_6 tag followed by a tobacco etch virus (TEV) cleavage site, was used to generate vectors for the DH-Ct, DH-Ext, and DH-PH His_6-tagged p63RhoGEF constructs. The p63RhoGEF DH construct was cloned into a His_6-tagged, TEV-cleavable, maltose-binding protein (MBP) fusion vector (pLiC-His-MBP-TEV) for improved expression and solubility. N-terminal glutathione *S*-transferase (GST)-tagged constructs for p63RhoGEF DH-Ext and DH-PH were cloned into a GST fusion vector using a similar strategy. Point mutant constructs of p63RhoGEF (F471A, L472A, N473A, L474A, Q476A, S477A, P478A, I479A, E480A, Y481A, Q482A, R483A) were generated in the context of the His_6-tagged DH-Ext using the Quik Change site-directed mutagenesis kit (Stratagene) followed by automated sequencing to confirm each mutation. The coding region for the C-terminal DH-Ext region of Trio (Trio-C DH-Ext, residues 1291–2299) was PCR amplified from full-length human Trio (Gen Bank accession number NM_007118, kindly provided by M. Strueli) and introduced into the pLiC-His-TEV bacterial expression vector as above. Baculovirus for the new $G\alpha_{i/q}$ chimera was constructed with the N-terminal His_6 tag followed by the N-terminal sequence of$G\alpha_{i1}$ (1–28), TEV cleavage site, and $G\alpha_q$ sequence starting at Ala^8. Baculovirus for the $G\alpha_{13}$ chimera was described in Ref. 32.

Protein Expression and Purification

All p63RhoGEF and Trio-C recombinant protein expression constructs were expressed in the BL21 (DE3) *Escherichia coli* strain. Cells were grown up at 37 °C in LB media containing 0.1 mg/ml ampicillin until an A_{600} of ~0.6, then induced with 0.1 mM isopropyl β-D-thiogalactopyranoside and grown up at 18 °C for ~18 h. Cells containing His_6-tagged proteins were harvested and soluble recombinant proteins were purified using standard Ni^{2+}-affinity chromatography followed by size-exclusion chromatography. Prior to size-exclusion chromatography, some His_6-tagged proteins were treated with TEV to remove the His_6 tag. Additionally, treatment with TEV allowed for removal of the N-terminal MBP fusion of the p63RhoGEFDHconstruct. *E. coli* cells containing GST fusion p63RhoGEF proteins (GST-DH-Ext, GST-DH-PH) were also harvested and recombinant proteins purified using standard glutathione-affinity chromatography followed by size-exclusion chromatography. Chimeric fusion constructs of the heterotrimeric G proteins $G\alpha_q$ and$G\alpha_{13}$ were purified using a baculovirus-based expression system (Invitrogen) in High-5 insect cells based on methods previously described (32,33). Purified protein samples for the heterotrimeric G proteins $G\alpha_i$, $G\alpha_o$, $G\alpha_t$, and $G\alpha_s$ were generously provided by C. Johnston and D. Siderovski (34,35). Heterotrimeric Gα-subunits were confirmed active using several independent methods including AlF_4-dependent binding to effectors proteins. Additionally, Dbs DH-PH (residues 623–967), Tiam1 DH-PH (residues 1022–1406), Rac1 (residues 1–189 C189S), Cdc42

NIH-PA Author Manuscript

NIH-PA Author Manuscript

NIH-PA Author Manuscript

(residues 1–189 C189S), RhoA (residues 1–190 C190S), RhoB (residues 1–190, C190S), and RhoC (residues 1–191, C191S) were expressed in *E. coli* and purified essentially as previously described (15,36,37). Size-exclusion chromatography was used for all recombinant protein preparations to ensure samples eluted as monodispersed species of correct molecular weight. All recombinant protein concentrations were determined using the A_{280} method with extinction coefficients calculated using the ProtParam tool (ExPASy Molecular Biology Server (38)), analyzed by SDS-PAGE to confirm concentration and ensure purity, and subsequently stored at −80 °C.

Guanine Nucleotide Exchange Assays

The guanine nucleotide exchange activity of purified RhoGEFs was determined using a kinetic, fluorescence-based assay with Rho GTPases (RhoA, RhoB, RhoC, Rac1, Cdc42) that were preloaded with BODIPY FL-conjugated GDP (BODIPY-GDP, Molecular Probes) essentially as previously described (39). All exchange assays were performed using an LS-55 fluorescence spectrometer (PerkinElmer) with wavelengths set at λ_{ex} = 500 nm (slits = 5 nm),λ_{em} = 511 nm (slits = 5 nm), and quartz cuvettes thermostatted at 20 °C while constantly stirred. Reactions were carried out in exchange buffer consisting of 20 mM Tris, pH 7.5, 200mM NaCl, 10mM $MgCl_2$, 5% (v/v) glycerol, and 10μM GDP. For each exchange assay, BODIPY-GDP-preloaded Rho GTPases (200 nM) were allowed to equilibrate in exchange buffer. Then 30μM AlF_4 (30μM $AlCl_3$+10mM NaF) and/or heterotrimeric G proteins at the indicated concentrations were added. The presence of AlF_4 had no impact on the spontaneous exchange rate of Rho GTPases and was used to selectively activate heterotrimeric G proteins. Finally, the guanine nucleotide exchange reaction was initiated by the manual addition of the RhoGEF at the indicated concentrations and the exchange reaction was monitored in real time until completion. The observed exchange rates (k_{obs}) were then calculated for each condition by fitting the change in relative fluorescence intensity over time for a given condition to a single-phase exponential decay using Prizm data analysis software (GraphPad). Exchange data depicted in bar graphs are the mean ± S.D. for each condition, conducted in triplicate. Representative real time kinetic exchange data depicted in curves are normalized as follows: relative fluorescence units prior to addition of RhoGEF (100% BODIPY-GDP bound) and relative fluorescence units at reaction completion (0% BODIPY-GDP bound).

Surface Plasmon Resonance Binding Studies

All surface plasmon resonance (SPR) studies were performed using a Biacore 3000 instrument (GE Healthcare). An anti-GST antibody was covalently coupled to a CM5 Biacore chip per the manufacturer's protocol. Binding studies were performed in SPR buffer consisting of 20 mM HEPES, pH 7.5, 150 mM NaCl, 10 mM $MgCl_2$, 0.05% (v/v) Nonidet P-40, 100 μM GDP, and 30 μM AlF_4 (30 μM $AlCl_3$ + 10 mM NaF). GST fusion binding surfaces were subsequently generated for individual flow cells by the application of GST only, or the GST-tagged p63RhoGEF constructs GST-DHExt and GST-DH-PH. To generate SPR-based binding isotherms, an analyte consisting of 10 μM $G\alpha_q$ in AlF_4-containing SPR buffer was flowed over each surface; background binding to the GST only surface was subsequently subtracted from each condition and the corresponding relative units were plotted.

Fluorescence Polarization Binding Studies

Apeptide spanning the conserved PH domain extension of p63RhoGEF was synthesized and high pressure liquid chromatography purified by the Tufts University peptide core facility. This peptide consisted of an N-terminal fluorescein moiety followed by a β-alanine linker and residues 467–493 of human p63RhoGEF followed by a C-terminal amide group. $G\alpha_q$ or $G\alpha_i$ were added at varying concentrations to a 96-well plate containing 5 nM peptide in buffer consisting of 20 mM Tris, pH 7.5, 200 mM NaCl, 20 mM $MgCl_2$, 0.05% (v/v) Nonidet P-40, 30

NIH-PA Author Manuscript

NIH-PA Author Manuscript

NIH-PA Author Manuscript

μM GDP, and 30 μM AlF_4 (30 $AlCl_3$+10mM NaF) with a total volume of 200μl. Each condition was allowed to equilibrate at 25 °C for ~15 min before polarization was determined using a PHERAstar fluorescence microplate reader (BMG Labtech) using the polarization mode. The excitation laser (λ_{ex} = 485 nm) was vertically polarized and the subsequent fluorescence emission intensity (λ_{em}= 520 nm) was observed through a polarizer orientated parallel or perpendicular to the excitation vector. Polarization (*P*) was then calculated using the formula: $p=(I_{\parallel}-I_{\perp})/(I_{\parallel}+I_{\perp})$, where $I_{\parallel}$is the intensity of the parallel component and $I_{\perp}$ is the intensity of the perpendicular component of the emitted light (40). Peptide in the absence of heterotrimeric G protein was used to adjust the gain prior to data collection.

RESULTS

Sequence Analysis Reveals a Highly Conserved Extension of the DH-associated PH Domain of p63RhoGEF

Unlike the majority of the 69 human Dbl-family GEFs, p63RhoGEF lacks any additional signaling domains outside of the canonical DH-PH cassette that defines this family. To identify conserved regions that may impart signaling properties or suggest modes of regulation for p63RhoGEF, we generated a multiple sequence alignment using Clustal-X (41) for eight representative p63RhoGEF orthologs and projected the sequence conservation for each residue onto the predicted domain architecture (Fig. 1*A*). The three-dimensional structure of PH domains is well characterized and takes on a β-sandwich fold capped on one side by a C-terminal α-helix, termed αC (17). Interestingly, the predicted αC helix of p63RhoGEF has a highly conserved extension, which is predicted to be unstructured and is not considered an integral part of the PH domain based on sequence analysis (Fig. 1*A*). The strict conservation of this region and its proximity to the PH domain led us to hypothesize that this unique extension may be essential for regulating the exchange activity of p63RhoGEF. Based on these sequence analysis studies, we generated several p63RhoGEF truncation mutant constructs (Fig. 1*A*) and purified recombinant protein components to near homogeneity for use in our subsequent biochemical/biophysical analyses (Fig. 1*B*).

The Guanine Nucleotide Exchange Activity of p63RhoGEF Is Autoinhibited by the DH-associated PH Domain

We tested p63RhoGEF truncation mutants for their ability to promote guanine nucleotide exchange using RhoA as a substrate GTPase to investigate the mechanism of autoregulation. The exchange activities of p63RhoGEF constructs encompassing the DH-Ct, DH-Ext, and DH-PH were similarly activating toward RhoA, yielding an ~2–3-fold increase in the exchange rate over the spontaneous exchange rate of RhoA alone (Fig. 2). Full-length p63RhoGEF was similar in its activation of RhoA (data not shown). These results rule out possible regulation by inhibitory sequences, which have been well characterized for Vav and more recently, Tim-family RhoGEFs (42). However, under identical conditions, the DH construct was ~22-fold more active than the spontaneous exchange rate of RhoA alone (Fig. 2), implicating the PH domain as a negative regulator of p63RhoGEF exchange activity. To generate a soluble p63RhoGEFDHfragment, we used a TEV-cleavable MBP fusion at the N terminus; both MBP fusion and TEV-treated DH constructs retained similar activity toward RhoA. Whereas there is conflicting literature regarding the regulatory role of the PH domain of p63RhoGEF, our results are in accordance with previous studies that suggest an autoinhibitory role (43,44).

Activated $G\alpha_q$ Directly Stimulates the Guanine Nucleotide Exchange Activity of p63RhoGEF

Whereas Lutz and colleagues (30) elegantly demonstrated that $G\alpha_{q/11}$ synergizes with p63RhoGEF to activate RhoA signaling pathways in cells, the authors did not explore the underlying mechanism. Therefore, we used previously published methods (33) to generate soluble recombinant $G\alpha_q$ protein to test the hypothesis that $G\alpha_q$ directly stimulates p63RhoGEF

NIH-PA Author Manuscript

NIH-PA Author Manuscript

NIH-PA Author Manuscript

activity. The new $G\alpha_{i/q}$ chimera contains the N-terminal α-helix of $G\alpha_{i1}$ followed by a TEV cleavage site fused to the N terminus of $G\alpha_q$-(8–359); treatment with TEV-generated recombinant soluble $G\alpha_q$ protein with amino acid sequence from Ala^8 to the end and was purified with high purity (Fig. 1*B*). In contrast to the previous $G\alpha_q$ chimera (33), this new chimera demonstrated phospholipase C-β stimulating activity *in vitro*.[5] Subsequently, we established that purified $G\alpha_q$ directly stimulates the exchange activity of autoinhibited p63RhoGEF (Fig. 3, *A* and *B*). The exchange activity of each p63RhoGEF truncation mutant construct in the presence of inactive GDP-bound $G\alpha_q$ or AlF_4 alone was comparable with the control exchange rate, comprising a 2–3-fold activation over the spontaneous exchange rate of RhoA alone. However, the DH-Ct and DH-Ext constructs of p63RhoGEF were robustly stimulated by AlF_4-activated $G\alpha_q$ by~26-fold over the spontaneous exchange rate of RhoA alone. Additionally, full-length p63RhoGEF was similarly activated by AlF_4-activated $G\alpha_q$; however, the purity of the full-length construct was diminished due to N-terminal degradation (data not shown). Interestingly, the DH-PH construct lacking the conserved extension of the PH domain was not stimulated by AlF_4-activated $G\alpha_q$. This lack of $G\alpha_q$-mediated stimulation of the DH-PH fragment was not simply due to misfolding as the basal activity closely resembled that of the DH-Ct and DH-Ext constructs. Additionally, the DH construct lacking the autoinhibitory PH domain was not further stimulated by addition of AlF_4-activated $G\alpha_q$ (Fig. 3*C*). Most likely, the DH construct represents constitutively active p63RhoGEF. The exchange rates catalyzed by p63RhoGEF (DH-Ext) in the presence of increasing amount of AlF_4-activated $G\alpha_q$ (Fig. 4*A*), were used to generate a dose-response curve that yielded an EC_{50} of ~951 n_M for the activation of p63RhoGEF by AlF_4-activated $G\alpha_q$ (Fig. 4*B*). Based on these results, the DH-Ext construct comprises the minimal region of p63RhoGEF that is both basally autoinhibited and activated by AlF_4-activated $G\alpha_q$; subsequent experiments utilized this DH-Ext construct.

Next, we identified key residues within p63RhoGEF essential for $G\alpha_q$-mediated activation using site-directed mutagenesis of the conserved PH domain extension (residues 466–483, alanine 474 was not mutated). In particular, alanine substitutions in the context of DH-Ext at Phe^{471}, Leu^{472}, Leu^{475}, Pro^{478}, and Ile^{479} substantially diminished the capacity for AlF_4-activated $G\alpha_q$ to stimulate the exchange activity of p63RhoGEF compared with wild-type (Fig. 5*A*). The basal exchange activity of these point mutants (*i.e.* in the absence of activated $G\alpha_q$) was comparable with the basal exchange activity of wild-type p63RhoGEF and proteins eluted as mono-dispersed species of correct molecular weight when analyzed by size-exclusion chromatography and SDS-PAGE (Fig. 5*C*), indicating proper folding and protein integrity. Interestingly, mutations most deleterious to $G\alpha_q$-mediated stimulation of p63RhoGEF display helical periodicity and appear to encompass the single face of an α-helix when analyzed using bioinformatics-based methods (ExPASy Molecular Biology Server (38)) (Fig. 5*B*). This was an unexpected finding as this region is predicted to be unstructured based on secondary structure prediction methods. We hypothesize that this normally disordered extension undergoes a conformational change to an α-helix upon binding $G\alpha_q$.

We then performed binding assays to determine whether this conserved extension was important for directly engaging activated $G\alpha_q$ or merely contributed to allosteric activation of the DH domain. We used both analytical size-exclusion chromatography (Fig. 6*A*) as well as SPR analysis (Fig. 6*B*) to show that the p63RhoGEF DH-Ext binds AlF_4-activated $G\alpha_q$ with a high affinity, whereas the DH-PH construct lacking the extension motif does not interact with activated $G\alpha_q$. Further analysis of the SPR-generated binding isotherms indicate that the DH-Ext construct bound activated $G\alpha_q$ with an association rate constant of 0.12 and a dissociation rate constant of 0.039. Whereas these results indicate that the C-terminal extension was

[5]T. Kawano and T. Kozasa, unpublished results.

NIH-PA Author Manuscript

NIH-PA Author Manuscript

NIH-PA Author Manuscript

necessary for binding activated $G\alpha_q$, they do not address whether it was sufficient for binding. Therefore we generated a peptide corresponding to the C-terminal extension of p63RhoGEF (residues 467– 493) and showed that this peptide was sufficient to bind AlF_4-activated $G\alpha_q$ using a polarization/anisotropy-based binding assay, whereas AlF_4-activated $G\alpha_i$ did not bind this peptide (Fig. 6*C*). However, the relatively low affinity for this interaction suggests to us that additional regions outside of this minimal peptide are required for full engagement of activated $G\alpha_q$ by p63RhoGEF.

G Protein Specificity Determinants for p63RhoGEF

To determine the full spectrum of heterotrimeric G proteins specific for p63RhoGEF, we tested a panel of highly purified recombinant Gα-subunits for their ability to directly stimulate the exchange activity of p63RhoGEF. As expected, the exchange activity of p63RhoGEF (DH-Ext) was not affected by the addition of high concentrations of AlF_4-activated $G\alpha_i$, $G\alpha_o$, $G\alpha_s$, $G\alpha_t$, and $G\alpha_{13}$ (Fig. 7*A*). The resulting exchange rates were comparable with that of the control exchange rate in the absence of heterotrimeric G proteins, comprising a 2–3-fold activation over the spontaneous exchange rate of RhoA alone. Only $G\alpha_q$ robustly stimulated the guanine nucleotide exchange activity in an AlF_4-dependent manner. Secondary studies, including AlF_4-dependent binding of effector proteins, were used to confirm the activity of each heterotrimeric G protein used (34,35); the purity and concentration of each heterotrimeric G protein used was additionally confirmed using SDS-PAGE analysis (Fig. 7*B*). Currently, we are developing baculoviral expression constructs to probe additional $G\alpha_q$ family members (*e.g.* $G\alpha_{11}$ and $G\alpha_{14}$) for activation of p63RhoGEF.

The substrate Rho GTPase specificity for p63RhoGEF has not been well characterized. Therefore, we investigated the substrate Rho GTPase specificities for $G\alpha_q$-activated p63RhoGEF. High concentrations of AlF_4-activated $G\alpha_q$ in combination with p63RhoGEF (DH-Ext) did not promote guanine nucleotide exchange on BODIPY-GDP-preloaded Rac1 (Fig. 7*C*) or Cdc42 (Fig. 7*D*). The activity of both Rac1 and Cdc42 were confirmed using the RhoGEFs Tiam1 and Dbs, respectively (Fig. 7, *C* and *D*). Additionally, we demonstrated that $G\alpha_q$-activated p63RhoGEF catalyzes guanine nucleotide exchange on Rho isozymes RhoB and RhoC (Fig. 7*E*). This activation of RhoB and RhoC by p63RhoGEF was comparable with that observed with RhoA, implicating p63RhoGEF as a Rho isoform-specific exchange factor.

The Rho-specific Exchange Activity of the C-terminal DH-PH Cassette of Trio Is Similarly Stimulated by Activated $G\alpha_q$

Because there is a large precedent for RhoA signaling downstream of $G\alpha_q$ we hypothesized additional Dbl-family members related to p63RhoGEF may also be directly by activated $G\alpha_q$. Therefore, we used the basic local alignment search tool (45) to identify additional proteins homologous to p63RhoGEF that may also interact directly with activated $G\alpha_q$. We identified the Dbl-family proteins Trio and Kalirin as the closest paralogs to p63RhoGEF. More importantly, Trio and Kalirin were the only other proteins that contain the highly conserved C-terminal extension of the PH domain (residues 471– 483), which is required for direct engagement of activated $G\alpha_q$ by p63RhoGEF. Trio and Kalirin are unique in that they are the only Dbl-family members that contain two independent DH-PH cassettes (14). The N-terminal DH-PH cassette is Rac1/RhoG-specific, whereas the C-terminal DH-PH cassette is RhoA-specific (46,47). Only the C-terminal RhoA-specific and not the N-terminal Rac1/RhoG-specific DH-PH cassette of Trio and Kalirin bear significant homology to p63RhoGEF (Fig. 8*A*). Interestingly, residues within the PH domain extension that were essential for p63RhoGEF activation by $G\alpha_q$ (Phe^{471}, Leu^{472}, Leu^{475}, Pro^{478}, and Ile^{479}) are 100% conserved in Trio and Kalirin. We subsequently determined that AlF_4-activated $G\alpha_q$ can directly stimulate the RhoA-specific guanine nucleotide exchange activity of the C-terminal DH-PH cassette of Trio (Trio-C DH-Ext) by ~2-fold over inactive GDP-bound $G\alpha_q$ or AlF_4 alone (Fig. 8, *B* and *C*). This

NIH-PA Author Manuscript

NIH-PA Author Manuscript

NIH-PA Author Manuscript

stimulation by $G\alpha_q$ was not nearly as robust as that seen for p63RhoGEF, suggesting that other mechanisms may facilitate the interaction of activated $G\alpha_q$ with Trio. Alternatively, Trio-C DH-Ext possesses a higher capacity to catalyze guanine nucleotide exchange upon RhoA relative to the equivalent fragment of p63RhoGEF. Therefore, AlF_4-activated $G\alpha_q$ is stimulating a form of Trio that is already highly exchange-competent such that the measured enhancement by $G\alpha_q$ belies the full potential of $G\alpha_q$ to activate full-length and, presumably, fully autoinhibited Trio.

DISCUSSION

There is considerable evidence suggesting that $G\alpha_{12/13}$ and $G\alpha_{q/11}$ family members independently activate RhoA signaling in response to extracellular stimuli (18,19,21,26–29). Whereas the $G\alpha_{q/11}$-specific pathway has remained poorly understood, numerous studies indicate that $G\alpha_{12/13}$ engage the RGS domain of the p115 family members and directly stimulate their RhoA-specific exchange activity (23). The p115 family RhoGEFs are the only Dbl-family members that contain an RGS domain; however, previous efforts to implicate p115 family members as $G\alpha_{q/11}$-responsive RhoGEFs have been largely unsuccessful. [6] The recent finding that $G\alpha_{q/11}$ synergizes with p63RhoGEF to promote Rho signaling in cells was significant given that $G\alpha_q$-responsive RhoGEFs have remained elusive. However, given that p63RhoGEF lacks any semblance of an effector-binding site for activated heterotrimeric G proteins, such as an RGS domain, there was no precedent for a direct mode of regulation. Here we provide evidence that $G\alpha_q$ directly engages and stimulates the Dbl-family member p63RhoGEF via novel mechanisms distinct from that previously described for the RGS containing RhoGEFs of the p115 family.

Like numerous Dbl-family members before it, p63RhoGEF was first identified during an oncogenic screen based on its ability to robustly transform NIH3T3 cells (48). An N-terminal truncation of p63RhoGEF that most likely arises by alternative splicing has been previously described in the literature as GEFT. GEFT lacks the first 106 amino acids, but is nevertheless, considered functionally redundant with the full-length protein, p63RhoGEF. Previous studies have implicated p63RhoGEF/GEFT in muscle regeneration and myogenesis (43), regulation of cardiac sarcomeric actin (49), cell proliferation and migration (50), dendritic spine formation (51), and neurite outgrowth (52). Collectively, these suggest p63RhoGEF is an important regulator of actin in excitatory tissues such as muscle and neurons. Interestingly, $G\alpha_q$-mediated activation of RhoA is also implicated in the pathophysiology of myocardial hypertrophy (6–8). Additional studies are needed to explore the contribution of p63RhoGEF to these and other physiological responses.

Our results support previous reports suggesting an autoinhibitory role for the PH domain of p63RhoGEF. Previous studies have demonstrated that the DH domain of p63RhoGEF activated serum response factor-dependent gene transcription more robustly than full-length protein (44). Previous work has also shown that the PH domain functioned in *trans* as a dominant-negative by reducing serum response factor-dependent gene transcription mediated by full-length (43) or isolated DH domains (44). However, conflicting reports also suggest the PH domain is essential for induction of stress fibers (49); additional studies may be needed to explore the membrane-targeting capacity of the PH domain and other associated *in vivo* roles.

We hypothesize that p63RhoGEF is autoinhibited in a manner analogous to that described for Sos1. The x-ray crystal structure of the Sos1 DH-PH cassette indicates that the PH domain folds back onto the DH domain, thereby occluding access to the Rho GTPase binding site and inhibiting activity (53). An extended linker region that joins the adjacent DH and PH domains

[6] R. J. Rojas and J. Sondek, unpublished results.

NIH-PA Author Manuscript

NIH-PA Author Manuscript

NIH-PA Author Manuscript

facilitates this intramolecular interaction within Sos1. However, p63RhoGEF bears no significant homology to the regions of Sos1 responsible for intramolecular binding.

Our results clarify conflicting literature regarding the Rho GTPase substrate specificity of p63RhoGEF. Previous reports suggest that p63RhoGEF is specific for RhoA in REF52 fibroblasts (49), H9C2 cardiomyocytes (49), J82 epithelial cells (44), and HEK-293 cells (30,44). Yet, other studies also characterized p63RhoGEF as specific for Rac1/Cdc42 in COS-7 and HeLa cells (50) or promiscuous for RhoA/Rac1/Cdc42 in C2C12 muscle cells (43) and N2A neuroblastoma cells (51,52). A high degree of cross-talk within the Rho subfamily typically complicates the interpretation of these cell-based specificity studies. Furthermore, previous *in vitro* analysis of p63RhoGEF specificity have relied on suboptimal methodology and have produced results suggesting either RhoA (44,49) or Rac1/Cdc42 specificity (50). Therefore, we performed *in vitro* characterization of substrate Rho GTPases using highly purified components with a robust real-time assay (39) to demonstrate that p63RhoGEF specifically activates the Rho isozymes RhoA, RhoB, and RhoC with similar potency. This result is in accordance with studies demonstrating the specific activation of RhoA, and not Rac1 or Cdc42, downstream of $G\alpha_{q/11}$ (18,19,21,26–29). Whereas the three Rho isozymes are highly homologous, recent evidence suggests they are not functionally redundant (54); additional studies are required to determine the functional relevance of RhoB/RhoC activation downstream of $G\alpha_{q/11}$ and p63RhoGEF. Interestingly, the p63RhoGEF gene, *GEFT*, bears the official moniker *RAC/CDC42 exchange factor*; our studies indicate this is a misnomer.

Based on sequence similarity, strict conservation of the PH domain extension, and evidence that Trio-C is directly stimulated by activated $G\alpha_q$ we hypothesize that p63RhoGEF, Trio, and Kalirin represent a novel subset of Dbl-family Rho-GEFs regulated by $G\alpha_{q/11}$. Trio and Kalirin share remarkable similarity with each other in their domain architecture and are both essential regulators of axon guidance and neuronal cell migration during neuronal development. A majority of studies on Trio and Kalirin have focused on the N-terminal Rac1/RhoG-specific DH-PH cassette; little is known about the C-terminal RhoA-specific DH-PH cassette. Interestingly, Trio-like proteins have been highly conserved throughout evolution. For example, the Trio orthologs in *Caenorhabditis elegans*, UNC-73, and *Drosophila*, d Trio, are essential for proper neuronal/axonal development (55,56). Whereas no current evidence directly implicates Trio and Kalirin in $G\alpha_{q/11}$-mediated signaling pathways, future studies in model organisms such as *Drosophila* and *C. elegans* may lend credence to this intriguing notion.

In summary, the studies presented here uncover a novel mode of regulation for Dbl-family GEFs by heterotrimeric G proteins and suggests that, in addition to p63RhoGEF, Kalirin and Trio may also signal downstream of $G\alpha_{q/11}$. Now, p63RhoGEF joins a small group of Dbl-family members that have been shown to be directly activated by heterotrimeric signaling components. Ongoing crystallographic studies within our group should soon uncover the molecular details underlying p63RhoGEF activation by $G\alpha_q$ at atomic resolution.

Acknowledgments

We are grateful to G. Waldo and A. Kimple for technical assistance, as well as C. Johnston and D. Siderovski for providing purified heterotrimeric G protein components. Additionally we are appreciative of plasmid DNA gifts from T. Weiland and M. Strueli.

REFERENCES

1. Burridge K, Wennerberg K. Cell 2004;116:167–179. [PubMed: 14744429]
2. Etienne-Manneville S, Hall A. Nature 2002;420:629–635. [PubMed: 12478284]
3. Hall A. Science 1998;279:509–514. [PubMed: 9438836]

NIH-PA Author Manuscript

NIH-PA Author Manuscript

NIH-PA Author Manuscript

4. Imamura F, Shinkai K, Mukai M, Yoshioka K, Komagome R, Iwasaki T, Akedo H. Int. J. Cancer 1996;65:627–632. [PubMed: 8598314]
5. Chatah NE, Abrams CS. J. Biol. Chem 2001;276:34059–34065. [PubMed: 11431481]
6. Aoki H, Izumo S, Sadoshima J. Circ. Res 1998;82:666–676. [PubMed: 9546375]
7. Hines WA, Thorburn A. J. Mol. Cell Cardiol 1998;30:485–494. [PubMed: 9515026]
8. Sah VP, Hoshijima M, Chien KR, Brown JH. J. Biol. Chem 1996;271:31185–31190. [PubMed: 8940118]
9. Fromm C, Coso OA, Montaner S, Xu N, Gutkind JS. Proc. Natl. Acad. Sci. U. S. A 1997;94:10098–10103. [PubMed: 9294169]
10. Martin CB, Mahon GM, Klinger MB, Kay RJ, Symons M, Der CJ, Whitehead IP. Oncogene 2001;20:1953–1963. [PubMed: 11360179]
11. Ueda H, Morishita R, Itoh H, Narumiya S, Mikoshiba K, Kato K, Asano T. J. Biol. Chem 2001;276:42527–42533. [PubMed: 11546796]
12. Ueda H, Morishita R, Narumiya S, Kato K, Asano T. Exp. Cell Res 2004;298:207–217. [PubMed: 15242775]
13. Vetter IR, Wittinghofer A. Science 2001;294:1299–1304. [PubMed: 11701921]
14. Rossman KL, Der CJ, Sondek J. Nat. Rev. Mol. Cell. Biol 2005;6:167–180. [PubMed: 15688002]
15. Rossman KL, Worthylake DK, Snyder JT, Siderovski DP, Campbell SL, Sondek J. EMBO J 2002;21:1315–1326. [PubMed: 11889037]
16. Chhatriwala MK, Betts L, Worthylake DK, Sondek J. J. Mol. Biol 2007;368:1307–1320. [PubMed: 17391702]
17. DiNitto JP, Lambright DG. Biochim. Biophys. Acta 2006;1761:850–867. [PubMed: 16807090]
18. Fukuhara S, Chikumi H, Gutkind JS. Oncogene 2001;20:1661–1668. [PubMed: 11313914]
19. Seasholtz TM, Majumdar M, Brown JH. Mol. Pharmacol 1999;55:949–956. [PubMed: 10347235]
20. Sah VP, Seasholtz TM, Sagi SA, Brown JH. Annu. Rev. Pharmacol. Toxicol 2000;40:459–489. [PubMed: 10836144]
21. Katoh H, Aoki J, Yamaguchi Y, Kitano Y, Ichikawa A, Negishi M. J. Biol. Chem 1998;273:28700–28707. [PubMed: 9786865]
22. Chen Z, Singer WD, Wells CD, Sprang SR, Sternweis PC. J. Biol. Chem 2003;278:9912–9919. [PubMed: 12525488]
23. Hart MJ, Jiang X, Kozasa T, Roscoe W, Singer WD, Gilman AG, Sternweis PC, Bollag G. Science 1998;280:2112–2114. [PubMed: 9641916]
24. Wells CD, Liu MY, Jackson M, Gutowski S, Sternweis PM, Rothstein JD, Kozasa T, Sternweis PC. J. Biol. Chem 2002;277:1174–1181. [PubMed: 11698392]
25. Nakamura S, Kreutz B, Tanabe S, Suzuki N, Kozasa T. Mol. Pharmacol 2004;66:1029–1034. [PubMed: 15258251]
26. Dutt P, Kjoller L, Giel M, Hall A, Toksoz D. FEBS Lett 2002;531:565–569. [PubMed: 12435612]
27. Chikumi H, Vazquez-Prado J, Servitja JM, Miyazaki H, Gutkind JS. J. Biol. Chem 2002;277:27130–27134. [PubMed: 12016230]
28. Vogt S, Grosse R, Schultz G, Offermanns S. J. Biol. Chem 2003;278:28743–28749. [PubMed: 12771155]
29. Barnes WG, Reiter E, Violin JD, Ren XR, Milligan G, Lefkowitz RJ. J. Biol. Chem 2005;280:8041–8050. [PubMed: 15611106]
30. Lutz S, Freichel-Blomquist A, Yang Y, Rumenapp U, Jakobs KH, Schmidt M, Wieland T. J. Biol. Chem 2005;280:11134–11139. [PubMed: 15632174]
31. Stols L, Gu M, Dieckman L, Raffen R, Collart FR, Donnelly MI. Protein Expression Purif 2002;25:8–15.
32. Kreutz B, Yau DM, Nance MR, Tanabe S, Tesmer JJ, Kozasa T. Biochemistry 2006;45:167–174. [PubMed: 16388592]
33. Tesmer VM, Kawano T, Shankaranarayanan A, Kozasa T, Tesmer JJ. Science 2005;310:1686–1690. [PubMed: 16339447]

NIH-PA Author Manuscript

NIH-PA Author Manuscript

NIH-PA Author Manuscript

34. Johnston CA, Willard FS, Jezyk MR, Fredericks Z, Bodor ET, Jones MB, Blaesius R, Watts VJ, Harden TK, Sondek J, Ramer JK, Siderovski DP. Structure 2005;13:1069–1080. [PubMed: 16004878]
35. Kimple RJ, De Vries L, Tronchere H, Behe CI, Morris RA, Gist Farquhar M, Siderovski DP. J. Biol. Chem 2001;276:29275–29281. [PubMed: 11387333]
36. Snyder JT, Worthylake DK, Rossman KL, Betts L, Pruitt WM, Siderovski DP, Der CJ, Sondek J. Nat. Struct. Biol 2002;9:468–475. [PubMed: 12006984]
37. Worthylake DK, Rossman KL, Sondek J. Nature 2000;408:682–688. [PubMed: 11130063]
38. Gasteiger E, Gattiker A, Hoogland C, Ivanyi I, Appel RD, Bairoch A. Nucleic Acids Res 2003;31:3784–3788. [PubMed: 12824418]
39. Rojas RJ, Kimple RJ, Rossman KL, Siderovski DP, Sondek J. Comb. Chem. High Throughput Screen 2003;6:409–418. [PubMed: 12769685]
40. Lakowicz, JR. Principles of Fluorescence Spectroscopy. Vol. 2nd Ed.. New York: Kluwer Academic/Plenum; 1999.
41. Thompson JD, Gibson TJ, Plewniak F, Jeanmougin F, Higgins DG. Nucleic Acids Res 1997;25:4876–4882. [PubMed: 9396791]
42. Yohe ME, Rossman KL, Gardner OS, Karnoub AE, Snyder JT, Gershburg S, Graves LM, Der CJ, Sondek J. J. Biol. Chem 2007;282:13813–13823. [PubMed: 17337446]
43. Bryan BA, Mitchell DC, Zhao L, Ma W, Stafford LJ, Teng BB, Liu M. Mol. Cell. Biol 2005;25:11089–11101. [PubMed: 16314529]
44. Lutz S, Freichel-Blomquist A, Rumenapp U, Schmidt M, Jakobs KH, Wieland T. Naunyn-Schmiedeberg's Arch. Pharmacol 2004;369:540–546.
45. Altschul SF, Gish W, Miller W, Myers EW, Lipman DJ. J. Mol. Biol 1990;215:403–410. [PubMed: 2231712]
46. Debant A, Serra-Pages C, Seipel K, O'Brien S, Tang M, Park SH, Streuli M. Proc. Natl. Acad. Sci. U. S. A 1996;93:5466–5471. [PubMed: 8643598]
47. Penzes P, Johnson RC, Kambampati V, Mains RE, Eipper BA. J. Neurosci 2001;21:8426–8434. [PubMed: 11606631]
48. Liu D, Yang X, Yang D, Songyang Z. Oncogene 2000;19:5964–5972. [PubMed: 11146547]
49. Souchet M, Portales-Casamar E, Mazurais D, Schmidt S, Leger I, Javre JL, Robert P, Berrebi-Bertrand I, Bril A, Gout B, Debant A, Calmels TP. J. Cell Sci 2002;115:629–640. [PubMed: 11861769]
50. Guo X, Stafford LJ, Bryan B, Xia C, Ma W, Wu X, Liu D, Songyang Z, Liu M. J. Biol. Chem 2003;278:13207–13215. [PubMed: 12547822]
51. Bryan B, Kumar V, Stafford LJ, Cai Y, Wu G, Liu M. J. Biol. Chem 2004;279:45824–45832. [PubMed: 15322108]
52. Bryan BA, Cai Y, Liu M. J. Neurosci. Res 2006;83:1151–1159. [PubMed: 16496360]
53. Soisson SM, Nimnual AS, Uy M, Bar-Sagi D, Kuriyan J. Cell 1998;95:259–268. [PubMed: 9790532]
54. Wheeler AP, Ridley AJ. Exp. Cell Res 2004;301:43–49. [PubMed: 15501444]
55. Bateman J, Van Vactor D. J. Cell Sci 2001;114:1973–1980. [PubMed: 11493634]
56. Rabiner CA, Mains RE, Eipper BA. Neuroscientist 2005;11:148–160. [PubMed: 15746383]

NIH-PA Author Manuscript

NIH-PA Author Manuscript

NIH-PA Author Manuscript

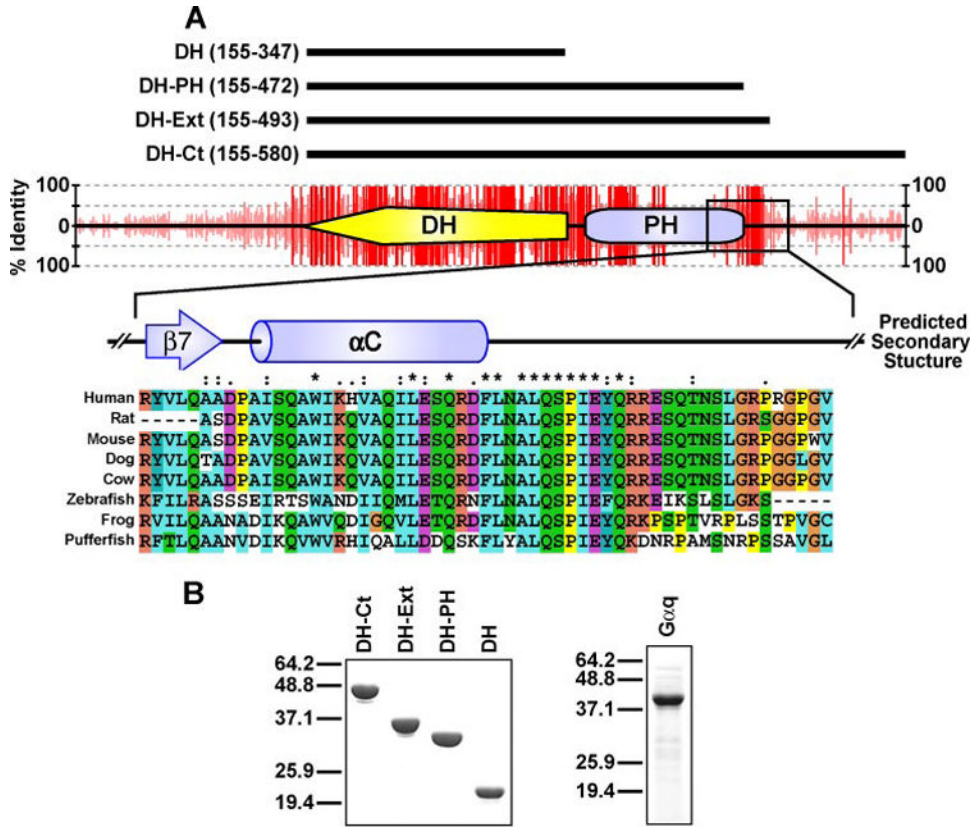

FIGURE 1. Sequence analysis of p63RhoGEF

A, a multiple sequence alignment for p63RhoGEF was generated from eight different species and used to calculate the percent identity for each residue using Clustal-X (41); these values are depicted as a *bar graph* projected onto the domain architecture of p63RhoGEF. The detailed portion of the multiple sequence alignment (spanning residues 443–499 of human p63RhoGEF) highlights a conserved extension to the C-terminal αC helix of the PH domain. Also shown is the predicted secondary structure for this region comprising the β7 β-sheet, αC α-helix, and unstructured regions depicted as a *black line*; truncation mutants generated for this study are also shown at the top with construct borders in *parentheses*. *B*, equal amounts (~5 μg) of purified protein components were analyzed by SDS-PAGE and stained with Coomassie Blue to confirm purity and concentration; molecular weight standards are also shown.

NIH-PA Author Manuscript

NIH-PA Author Manuscript

NIH-PA Author Manuscript

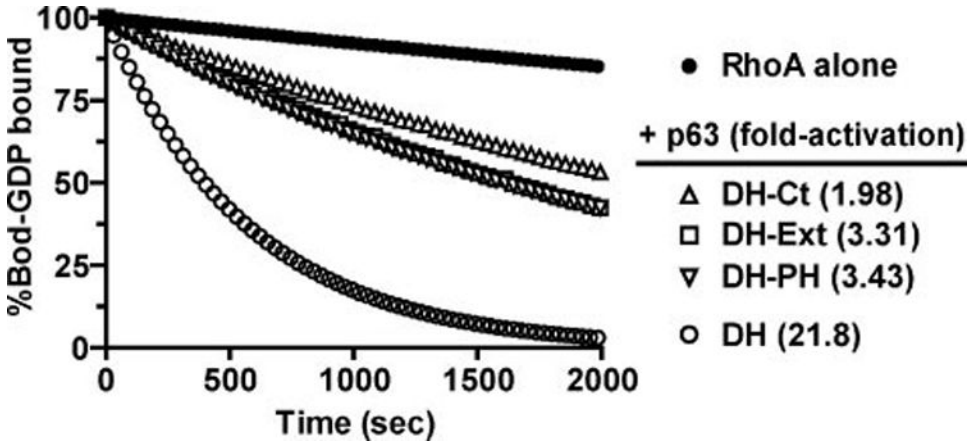

FIGURE 2. The PH domain negatively regulates the exchange activity of p63RhoGEF

RhoA alone, spontaneous nucleotide exchange of 200 nM BODIPY-GDP-preloadedRhoAin the absence of p63RhoGEF; *all others*, 200 nM of the indicated p63RhoGEF truncation mutant was added to 200 nM BODIPYGDP- preloaded RhoA to initiate guanine nucleotide exchange. Also shown is the calculated fold-activation over RhoA alone for each construct. All *curves* are representative of experiments performed in triplicate. *Bod*, BODIPY.

NIH-PA Author Manuscript

NIH-PA Author Manuscript

NIH-PA Author Manuscript

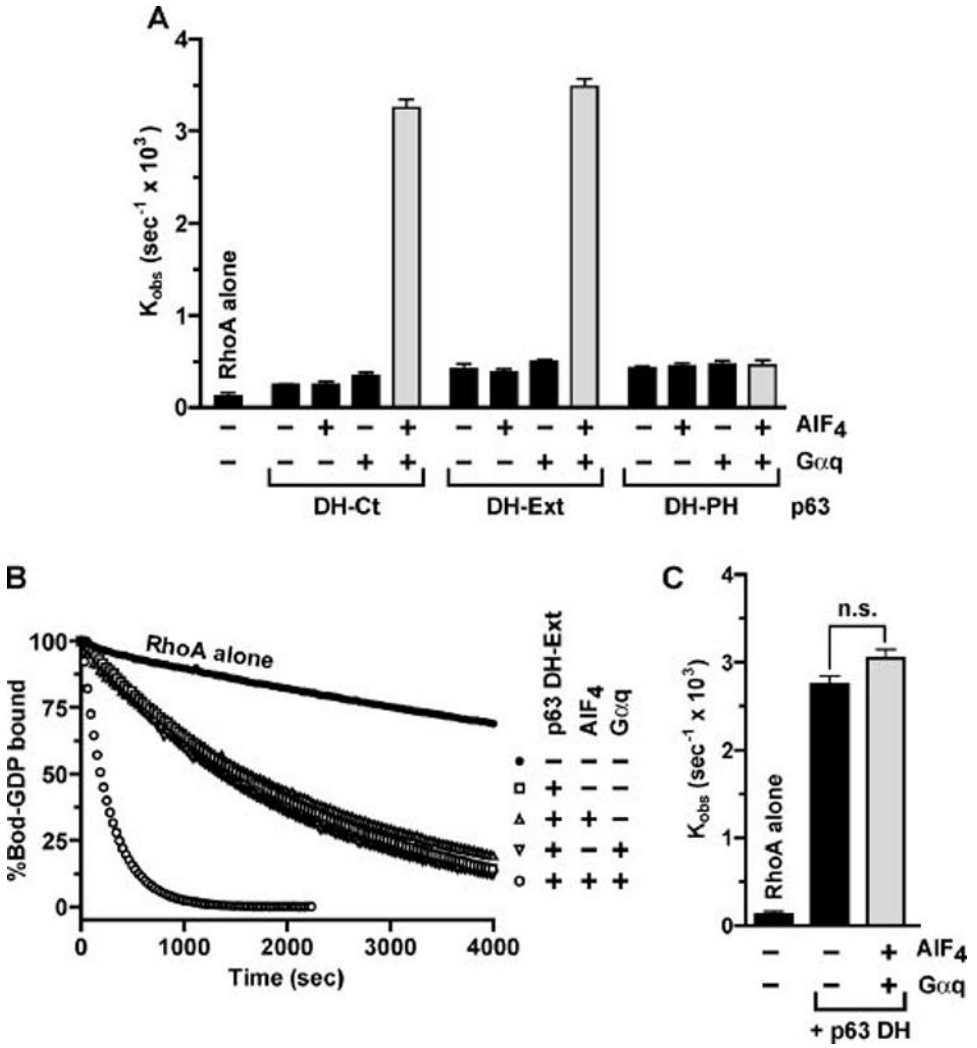

FIGURE 3. Gα_q directly stimulates the exchange potential of p63RhoGEF

A, RhoA alone, spontaneous nucleotide exchange of RhoA in the absence of p63RhoGEF; *all others*, 200 nM of the indicated p63RhoGEF truncation mutant was added to 200 nM BODIPY-GDP-preloaded RhoA in the presence or absence of 30μM AlF_4 and 200 nM $G\alpha_q$. *Bar graphs* depict the mean±S.D. for each condition conducted in triplicate. *B*, representative real-time kinetic data for the DH-Ext construct used to calculate exchange rates. *C*, the exchange activity of 200 nM p63RhoGEF DH upon 200 nM BODIPY-GDP-preloaded RhoA in the presence and absence of 200 nM AlF_4-actived $G\alpha_q$; shown is the mean ± S.D., *n.s.*, not significant by pairwise *t* test. *Bod*, BODIPY.

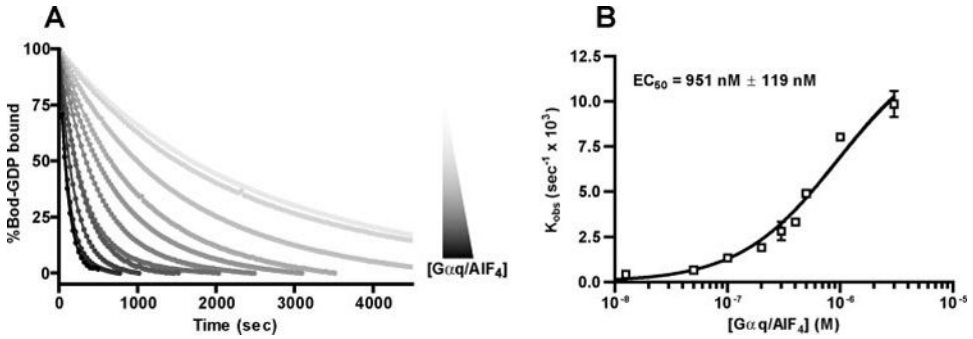

FIGURE 4. Dose-response curve for Gα_q-mediated stimulation of p63RhoGEF

A, the guanine nucleotide exchange activity of 200 nM p63RhoGEF (DH-Ext) upon 200 nM BODIPY-GDP-preloaded RhoA was determined in the presence of increasing amounts of AlF_4-activated $G\alpha_q$ (6.25 nM to 5 μM); shown are representative traces for each concentration used. *B*, the calculated exchange rates (k_{obs}) were plotted against $G\alpha_q$ concentration and fit to a one-site binding curve; data are the mean ± S.D. of two independent experiments. *Bod*, BODIPY.

NIH-PA Author Manuscript NIH-PA Author Manuscript NIH-PA Author Manuscript

NIH-PA Author Manuscript

NIH-PA Author Manuscript

NIH-PA Author Manuscript

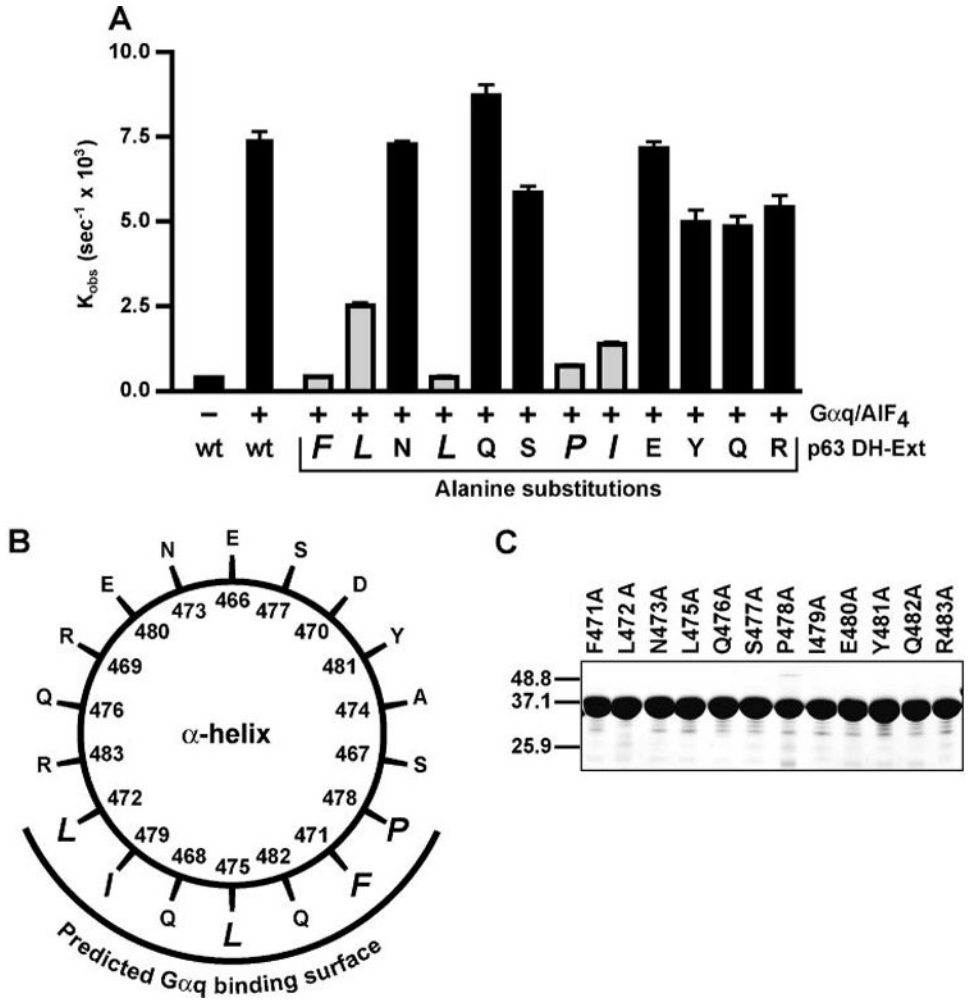

FIGURE 5. Mutational analysis of the conserved PH domain extension within p63RhoGEF

A, alanine substitutions were made within the conserved PH domain extension of p63RhoGEF in the context of DH-Ext. 200 nM of each point mutant was added to 200 nM BODIPY-GDP-preloaded RhoA in the presence of 300 nM $G\alpha_q$ and 30 μM AlF_4 prior to measuring exchange rates; the exchange activity of 200 nM wild-type (*wt*) p63RhoGEF (DH-Ext) in the presence and absence of 300 nM $G\alpha_q$ and 30 μM AlF_4 is also shown. *Bar graphs* depict the mean ± S.D. for the calculated exchange rate of each condition, conducted in triplicate; the most deleterious point mutants are highlighted. *B*, sequence containing the conserved PH domain extension (residues 466– 483, ESQRDFLNALQSPIEYQR) was modeled as an α-helix and displayed as a helical wheel (ExPASy Molecular Biology Server (38)) with the corresponding residue numbers, highlighted is the region predicted to bind $G\alpha_q$. *C*, equal amounts (~10 μg) of purified p63RhoGEF point mutants used in *A* were analyzed by SDS-PAGE and stained with Coomassie Blue to confirm purity and concentration; molecular weight standards are also shown (note that alanine 474 was not mutated).

NIH-PA Author Manuscript

NIH-PA Author Manuscript

NIH-PA Author Manuscript

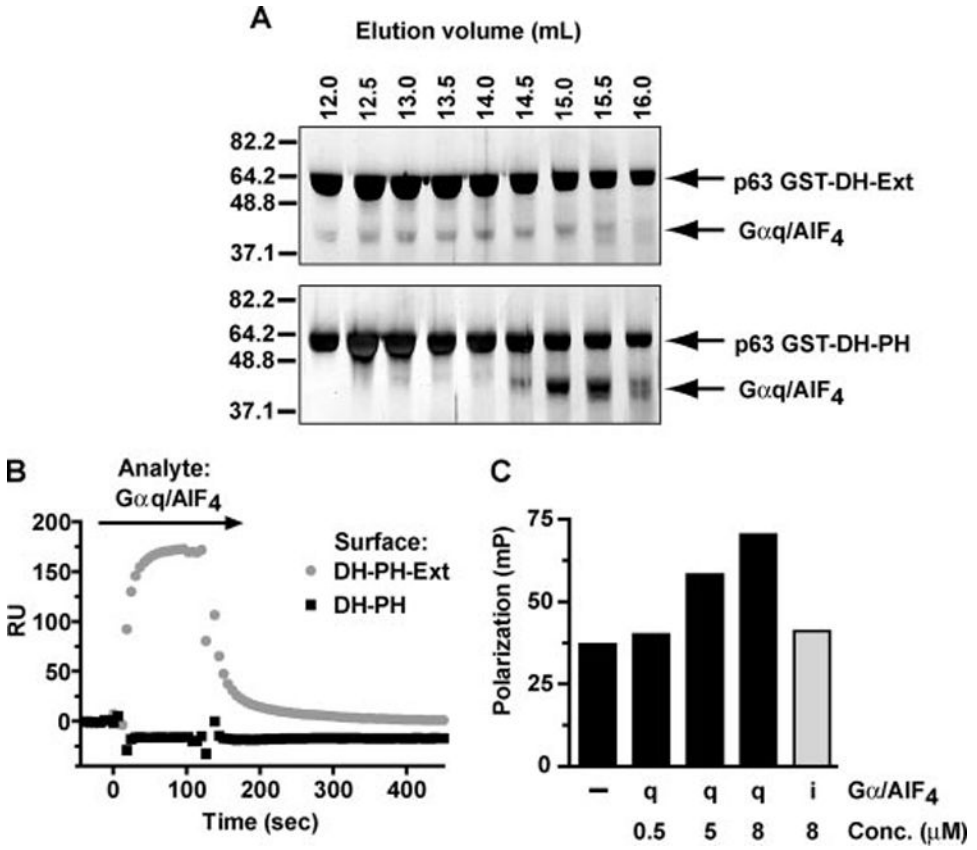

FIGURE 6. The conserved PH domain extension of p63RhoGEF is essential for direct binding of activated $G\alpha_q$

A, analytical gel-exclusion chromatography was used to isolate a heterodimeric complex of AlF_4-activated $G\alpha_q$ with GST-tagged p63RhoGEF (GST-DH-Ext); under identical conditions the GST-DH-PH construct did not complex with AlF_4-activated $G\alpha_q$ (*lower panel*). *B*, GST-tagged p63RhoGEF truncation constructs (GSTDH- Ext and GST-DH-PH) were immobilized onto the surface of the Biacore chip; analyte consisting of 10 μM AlF_4-activated $G\alpha_q$ was then flowed over each surface while measuring surface plasmon resonance. *C*, a fluorophore-conjugated peptide corresponding to the conserved PH domain extension of human p63RhoGEF (residues 467– 493) was used in a polarization/anisotropy-based assay to show direct dose-dependent binding to AlF_4-activated $G\alpha_q$.

NIH-PA Author Manuscript
NIH-PA Author Manuscript
NIH-PA Author Manuscript

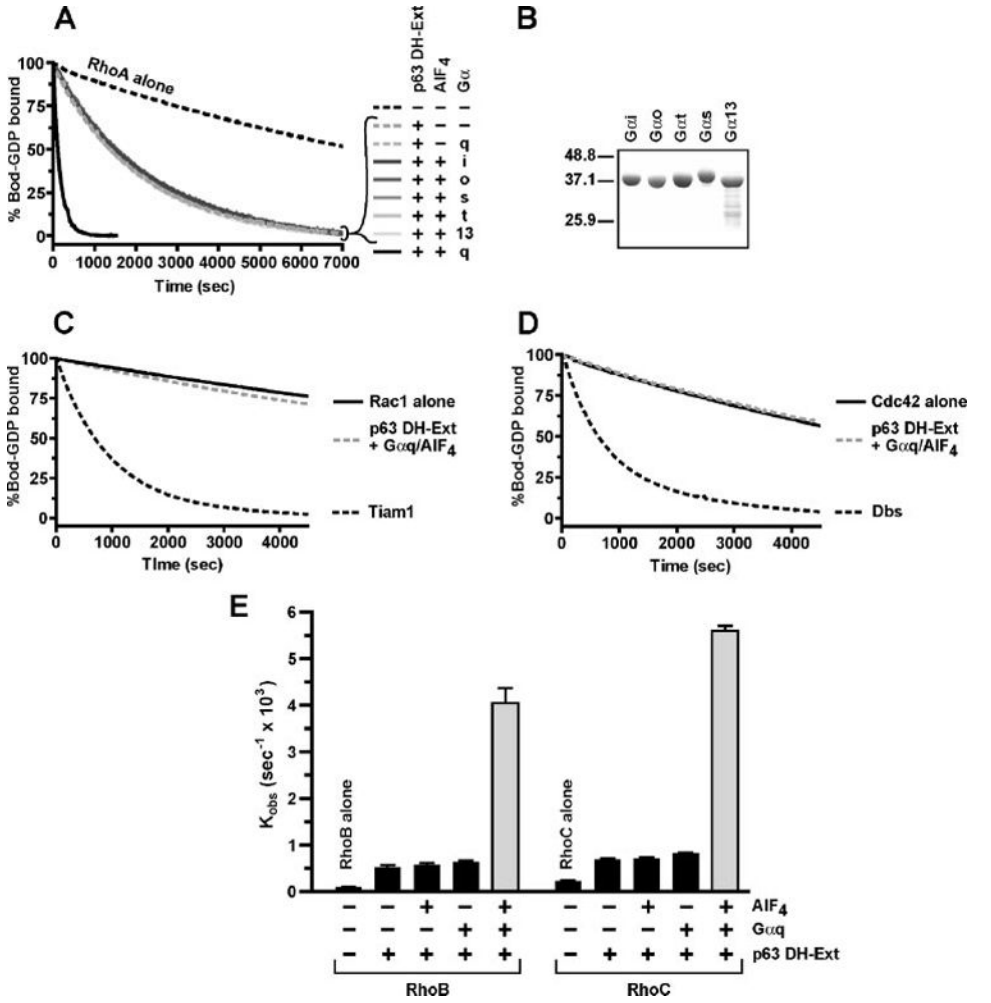

FIGURE 7. Specificity of p63RhoGEF for heterotrimeric Gα-subunits and substrate Rho GTPases

A, 200 nM p63RhoGEF (DH-Ext) was added to mixtures containing 200 nM BODIPY-GDP-preloaded RhoA in the presence or absence of 30 μM AlF_4 and 500 nM of the indicated Gα-subunit ($G\alpha_q$, $G\alpha_i$, $G\alpha_o$, $G\alpha_s$, $G\alpha_t$, and $G\alpha_{13}$). *B*, equal amounts (~5μg) of purified heterotrimeric G protein components used in *A* were analyzed by SDS-PAGE and stained with Coomassie Blue to confirm purity and concentration; molecular weight standards are also shown. *C* and *D*, 500 nM p63RhoGEF (DH-Ext), 500 nM $G\alpha_q$, and 30αM AlF_4 were added to reaction mixtures containing 200 nM BODIPY-GDP-preloaded Rac1 (*C*) and Cdc42 (*D*). 500 nM Tiam1 (DH-PH) was added to cand 50 nM Dbs (DH-PH) was added to dto confirm Rac1 and Cdc42 activity, respectively. *E*, *RhoB alone*, *RhoC alone*, spontaneous nucleotide exchange in the absence of p63RhoGEF; all others, 200 nM p63RhoGEF (DH-Ext) was added to reaction mixtures containing 200 nM BODIPY-GDP-preloaded RhoB or RhoC in the presence or absence of 30 μM AlF_4 and 200 nM $G\alpha_q$. *Bar graphs* depict the mean ± S.D. for the calculated exchange rate (k_{obs}) of each condition, conducted in triplicate. *Bod*, BODIPY.

NIH-PA Author Manuscript

NIH-PA Author Manuscript

NIH-PA Author Manuscript

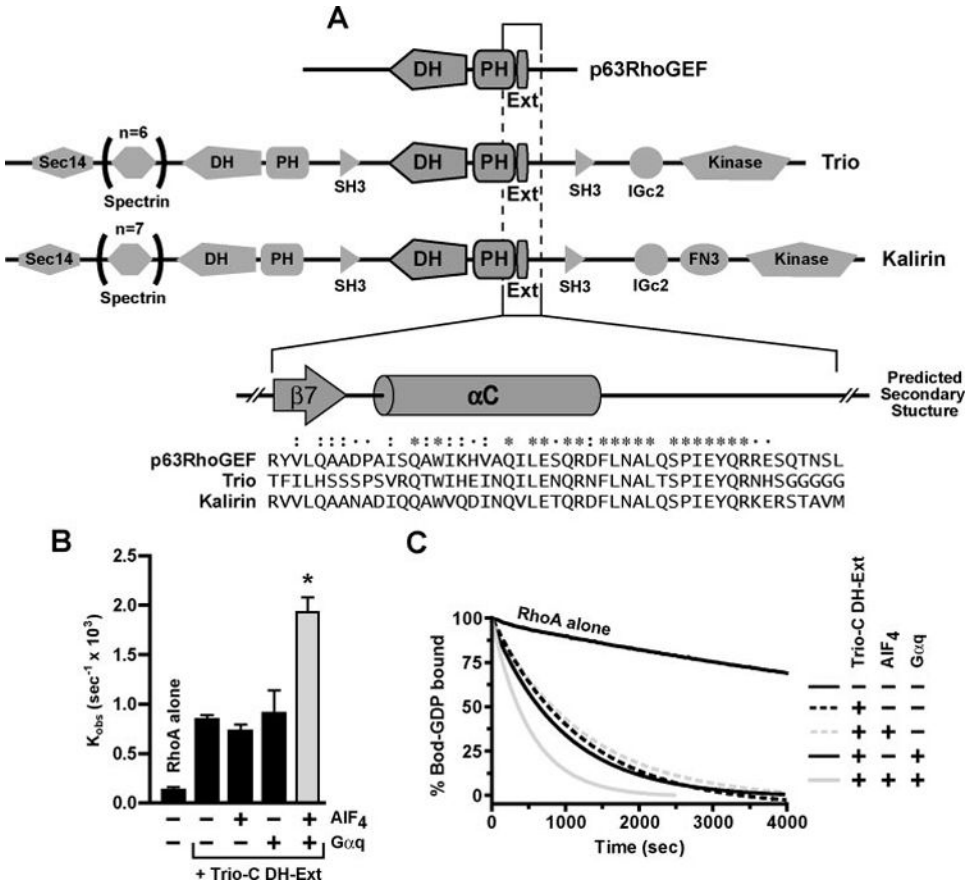

FIGURE 8. Gα_q directly stimulates the guanine nucleotide exchange activity of Trio-C

A, domain architecture of p63RhoGEF and its closest paralogs, Trio and Kalirin and multiple sequence alignment of the highly conserved C-terminal extension of the PH domain; also shown is the predicted secondary structure for the region of the PH domain proximal to the extension motif (β7,β-*sheet*;α*C*, *C-terminal*α-*helix*; *black line*, *unstructured*). *B*, the guanine nucleotide exchange assay was used to determine the exchange potential (k_{obs}) of Trio in response to AlF_4-activated $G\alpha_q$. *RhoA alone*, spontaneous nucleotide exchange for 200 nM BODIPY-GDP-loaded RhoA in the absence of Trio; all others, 200 nM Trio (DH-Ext) was added to 200 nM BODIPY-GDP-loaded RhoA in the presence or absence of 30 μM AlF_4 and 2 μM $G\alpha_q$ as indicated. *Bar graphs* depict the mean ± S.D. for the calculated exchange rate (k_{obs}) of each condition, conducted in triplicate; *asterisk* (*) denotes $p < 0.02$ compared with no$G\alpha_q$/AlF_4 present by pairwise *t* test. *C*, representative real-time kinetic data used to calculate exchange rates in *B*. *Bod*, BODIPY.